

## DIFFUSION RADIUS OF TRIPLE JUNCTIONS OF TILT BOUNDARIES IN Ni

G.M. Poletaev<sup>1\*</sup>, D.V. Novoselova<sup>1</sup>, I.V. Zorya<sup>2</sup>, M.D. Starostenkov<sup>1</sup>

<sup>1</sup>Altai State Technical University, Lenin Str. 46, Barnaul, 656038, Russia

<sup>2</sup>Siberian State Industrial University, Kirova Str. 42, Novokuznetsk, 654007, Russia

\*e-mail: gmpoletaev@mail.ru

**Abstract.** In the present study it was evaluated the diffusion radius of triple junctions of  $\langle 111 \rangle$  and  $\langle 100 \rangle$  tilt boundaries in Ni, obtained by crystallization, depending on the content of free volume. It is shown that diffusion in the area of triple junctions containing excess free volume proceeds much more intense than in the case when the additional vacancies were not introduced in the calculation block. In the  $\langle 100 \rangle$  boundaries and junctions formed by them during crystallization the free volume dissipated much more efficiently than in the junctions formed by the  $\langle 111 \rangle$  boundaries. For this reason the diffusion radius of the triple junction of  $\langle 100 \rangle$  boundaries at the introduction of 2 % conditional vacancies (about 3.5 Å) less than the radius of the junction of  $\langle 111 \rangle$  boundaries (4-5 Å).

### 1. Introduction

The triple junction of grains is a linear defect, along which three variously oriented grains or three grain boundary surfaces are conjugated. According to numerous experimental data, the diffusion along the triple junction proceeds more intensively than along the grain boundaries [1, 2], and the triple junction is often characterized by relatively "loose" structure [3] (even with inclusion of the amorphous phase [4]) with a higher content of free volume compared with the grain boundaries forming the junction.

In [5] with the help of computer simulation we have analyzed various causes of the formation of free volume in the triple junctions and concluded that the excess free volume forms in the junctions mainly during crystallization process in the result of "locking" of the liquid phase density at a meeting of the three crystallization fronts and, as a consequence, of the concentration of excess free volume in the triple junction after solidification. Accumulation of Burgers vector at the grain boundary sliding and the formation of dislocation or disclination complex in the junction we seem secondary cause.

The present work is devoted to the study by the method of molecular dynamics of self-diffusion and determination of the diffusion radius, i.e. the effective radius of the diffusion channel, of triple junctions containing excess free volume of  $\langle 111 \rangle$  and  $\langle 100 \rangle$  tilt boundaries in Ni. Nickel is selected as the well-studied typical fcc metal. The radius of the triple junction can be determined by the distribution in space of a local property (the potential energy distribution, diffusion permeability etc.) that allocated defect area on a background of pure crystal. Earlier, in [6], we carried out a similar study of the effective radius of triple junctions by the distribution of potential energy. It was shown that in the  $\langle 100 \rangle$  boundaries and junctions formed by them during crystallization the free volume dissipated much more efficiently than in the junctions formed by the  $\langle 111 \rangle$  boundaries. For the same reason effective energy radius of the triple junction of  $\langle 100 \rangle$  boundaries with the growth of

introduced free volume changes little: from 5 to 6 Å, when the radius of the junction of  $\langle 111 \rangle$  boundaries at a content 2 % of conditional vacancies may reach 14 Å.

## 2. Description of the model

The simulation was held using the method of molecular dynamics. The triple junctions of tilt boundaries with misorientation axes  $\langle 111 \rangle$  and  $\langle 100 \rangle$  were considered. The triple junction was formed in a center of the computational block by means of conjugation of three grains misoriented relative to each other using the rotation around the axis parallel to the line of the triple junction. In this study, the angles between the boundaries in the junction were specified to be equal to  $120^\circ$ . After cutting the segments, the conjugation of the grains was performed, during which the atoms situating at a distance shorter than 0.5 Å from the neighboring atom were removed. The final stage was cutting the final cylinder-shaped computational block. The example of the computational block with 60 Å radius formed as a result of the above described procedures is depicted in Fig. 1. The periodic boundary conditions were specified at the cylinder ends (infinite repetition of the cylindrical computational block along axis Z was specified). The rigid conditions were specified at the side cylinder surface, and the atoms near the side surface were not allowed to move during the computer experiment (in Fig. 1, the rigidly fastened atoms are shown dark gray). In this paper we considered the triple junction of  $\langle 111 \rangle$  tilt boundaries with misorientation angles between the three grains of  $15^\circ$ ,  $15^\circ$ ,  $30^\circ$  and  $\langle 100 \rangle$  tilt boundaries with misorientation angles of  $18^\circ$ ,  $18^\circ$ ,  $36^\circ$ .

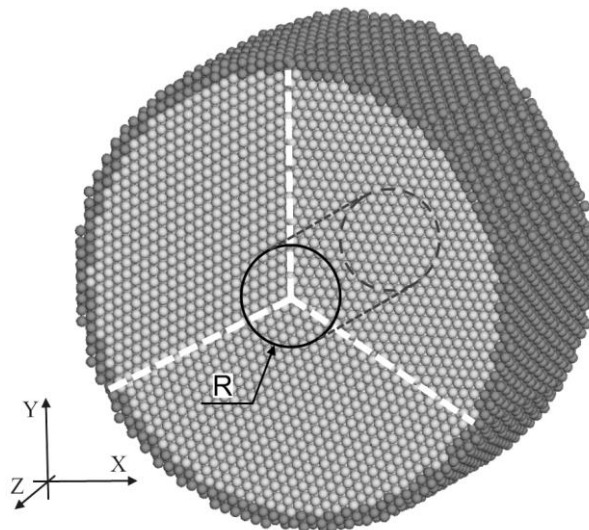


**Fig. 1.** Example of computational block with 60 Å radius containing the triple junction of  $\langle 111 \rangle$  tilt boundaries with  $15^\circ$ ,  $15^\circ$ ,  $30^\circ$  misorientation angles. The atoms that are shown dark gray remained immobile during the computer experiment (the rigid boundary conditions). The periodic boundary conditions were specified at the cylinder ends. The grain boundaries are denoted by the bright dashed lines. The area of radius  $R$  to calculate the diffusion coefficient along the triple junction is allocated in the figure.

The interactions of nickel atoms with each other were described by the Cleri-Rosato potential [7]. The potential developed by Cleri and Rosato within the tight-binding model have proven themselves in the molecular dynamics simulation of metallic systems and have been more successful test in many parameters [7-10]. The time integration step in the molecular dynamics method was equal 5 fs. Temperature in the model was set by changing the velocity of atoms in accordance with the Maxwell-Boltzmann distribution.

The next stage of preparation of the computational block was its melting, the introduction of free volume and subsequent crystallization. The computational block is heated

to a temperature well above the melting point (3000 K). After the simulated polycrystal became liquid, the thermostat was switched in the model and maintaining at a constant temperature below the melting temperature was conducted. Rigid boundaries (i.e. atoms rigidly fixed on the side surface of the cylindrical calculation block) simulated in this case crystallization fronts from three centers of crystallization (crystal clusters – fetuses of the solid phase). In [5] we showed that an important circumstance at the meeting of three crystallization fronts is the "locking" of the density in the area of the triple junction - the density of liquid phase remaining in the junction area, which has not yet crystallized, is lower than the density of the crystal phase. This lack of atoms to form an "ideal" triple junction leads to the appearance of excess free volume which is concentrated at the crystallization process preferably in the triple junction.

The free volume formed in the junction was calculated. It was shown that the concentration of conditional vacancies (i.e. the proportion of missing atoms compared with equilibrium triple junctions) can reach 2 % in the junction area. The junctions obtained as a result of crystallization of calculation blocks containing different amounts of conditional vacancies, from 0 % to 2 % (600 conditional vacancies per 30000 atoms), were considered in the present work.

The computational blocks obtained by above-described method were the starting in computer experiments on modeling of self-diffusion in area of the triple junctions.

### 3. Results and discussion

Figures 2 and 3 show the pictures of atomic displacements in the projection on XY plane (perpendicular to the junction line) in the area of junction of  $\langle 100 \rangle$   $18^\circ/18^\circ/36^\circ$  (Fig. 2) and  $\langle 111 \rangle$   $15^\circ/15^\circ/30^\circ$  (Fig. 3) tilt boundaries during the computer simulation for 150 ps at temperature of 1500 K in cases when the vacancies were not introduced into the computational block (Fig. 2a and 3a) and when it was introduced 2 % of conditional vacancies (Fig. 2b and 3b).

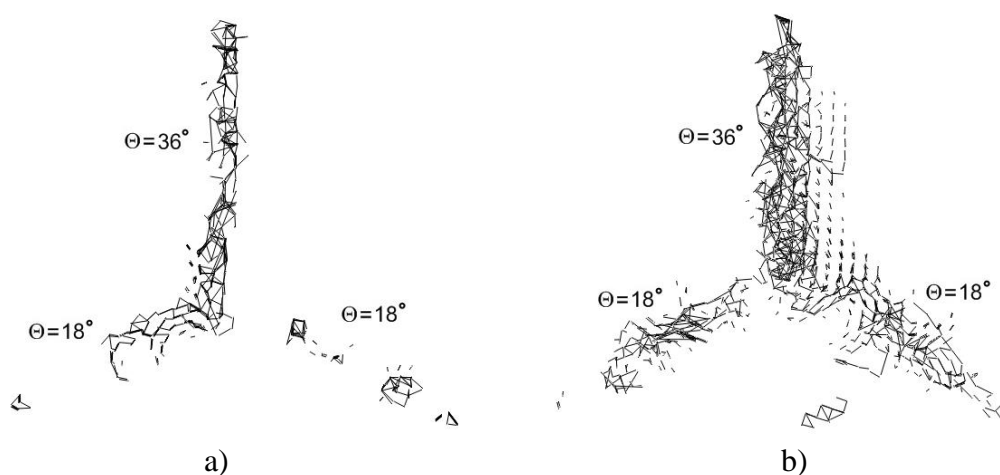


**Fig. 2.** Atomic displacements in projection on XY plane (depicted by segments) near the triple junction of  $\langle 100 \rangle$  tilt boundaries with  $18^\circ$ ,  $18^\circ$ ,  $36^\circ$  misorientation angles during computer simulation for 150 ps at temperature of 1500 K: a) the vacancies were not introduced into the starting computational block; b) 2 % of conditional vacancies was introduced. Displacements less than  $0.7 \text{ \AA}$  are not shown.

In cases when additional free volume was not introduced (Fig. 2a and 3a) the diffusion displacements of atoms in spite of the high temperature occurred in relatively narrow channels along the grain boundaries having (according to the received pictures) visual diffusion width of the order  $5 \text{ \AA}$ . This is in accordance with the conventional width of grain

boundaries [11, 12]. For  $\langle 100 \rangle$   $18^\circ$  (Fig. 2a) and  $\langle 111 \rangle$   $15^\circ$  (Fig. 3a) tilt boundaries it can clearly be seen "pipe" diffusion (diffusion along grain boundary dislocations) typical for low-angle tilt boundaries [13], which has significantly lower intensity than along the high-angle boundaries:  $\langle 100 \rangle$   $36^\circ$  and  $\langle 111 \rangle$   $30^\circ$ .

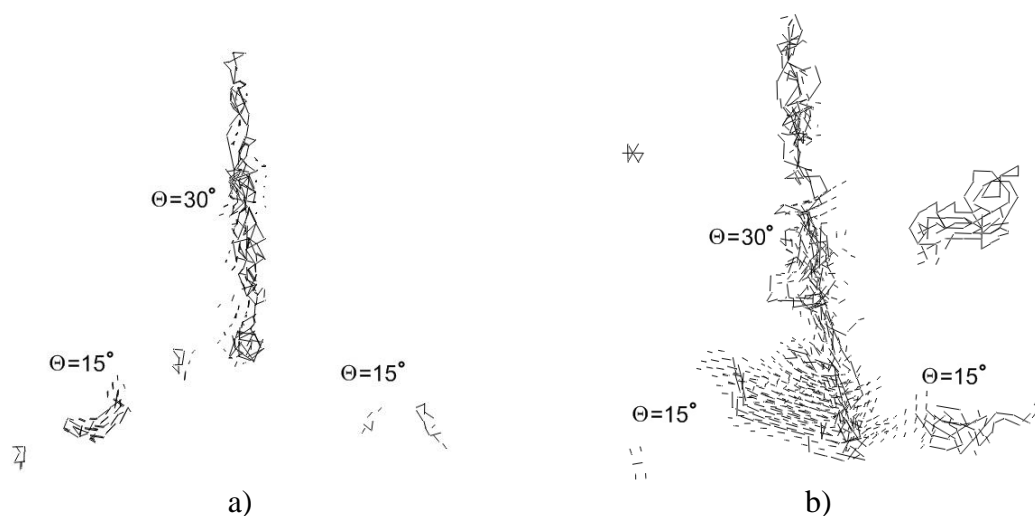


**Fig. 3.** Atomic displacements in projection on XY plane (depicted by segments) near the triple junction of  $\langle 111 \rangle$  tilt boundaries with  $15^\circ$ ,  $15^\circ$ ,  $30^\circ$  misorientation angles during computer simulation for 150 ps at temperature of 1500 K: a) the vacancies were not introduced into the starting computational block; b) 2 % of conditional vacancies was introduced. Displacements less than  $0.7 \text{ \AA}$  are not shown.

It can be seen on the above pictures of atomic displacements that in the triple junctions containing excess free volume the diffusion is considerably more intense than in the case when additional vacancies is not introduced into the computational block. The radius of the triple junction, as can be seen from Fig. 2 and 3, is the conventional concept – free volume is not concentrated locally in the center of the junction, but also distributed in the grain boundaries adjacent to the junction.

In addition to the displacements of atoms along the grain boundaries and triple junctions there are displacements in the grains in Fig. 2b and 3b. This is due to the fact that some amount of vacancies formed in the grains during crystallization.

To study the diffusion radius of triple junctions the self-diffusion coefficient values along the junctions were obtained depending on the radius of the calculation area  $R$  (Fig. 1). For triple junctions, taking into account the fact that the diffusion flux occurred along the axis of the cylindrical computational block, evaluation was performed by the coefficient of self-diffusion along the axis  $Z$ :

$$D_z = \frac{1}{2Nt} \sum_{i=1}^N (z_{0i} - z_i)^2.$$

Here  $z_{0i}$  and  $z_i$  – starting and ending  $Z$  axis coordinates of the  $i$ -th atom;  $N$  – number of atoms in the calculation area;  $t$  – time of the computer experiment.

Calculation area at determining of the coefficient of diffusion along the triple junction had the shape of a cylinder of radius  $R$  and length of the computational block (Fig. 1). In the computer program, it was possible to combine the center of the calculation area (the axis of cylinder) with a line of the triple junction based on the obtained in the simulation picture of atomic displacements.

Figure 4 shows the dependences of self-diffusion coefficient  $D_z$  along the considered triple junctions on radius  $R$  of the calculation area at temperature of 1500 K. Obtained

dependences  $D_z(R)$  have common features. Firstly, in all cases the self-diffusion coefficient increases with decreasing of radius  $R$ . This indicates that the diffusion flux is concentrated in a relatively narrow area located along the junction line. At that, than the higher values the diffusion coefficient  $D_z$  reaches with decreasing of radius  $R$ , the narrower is the diffusion channel.

With the introduction of 2 % of vacancies before the crystallization, as can be seen on the pictures of the atomic displacements above, the triple junction area more blurred and the junction has a larger radius. The diffusion coefficient along the junction of  $\langle 111 \rangle$  tilt boundaries takes smaller values in the area of the junction which is due to the relatively more "blurriness" of the junction.

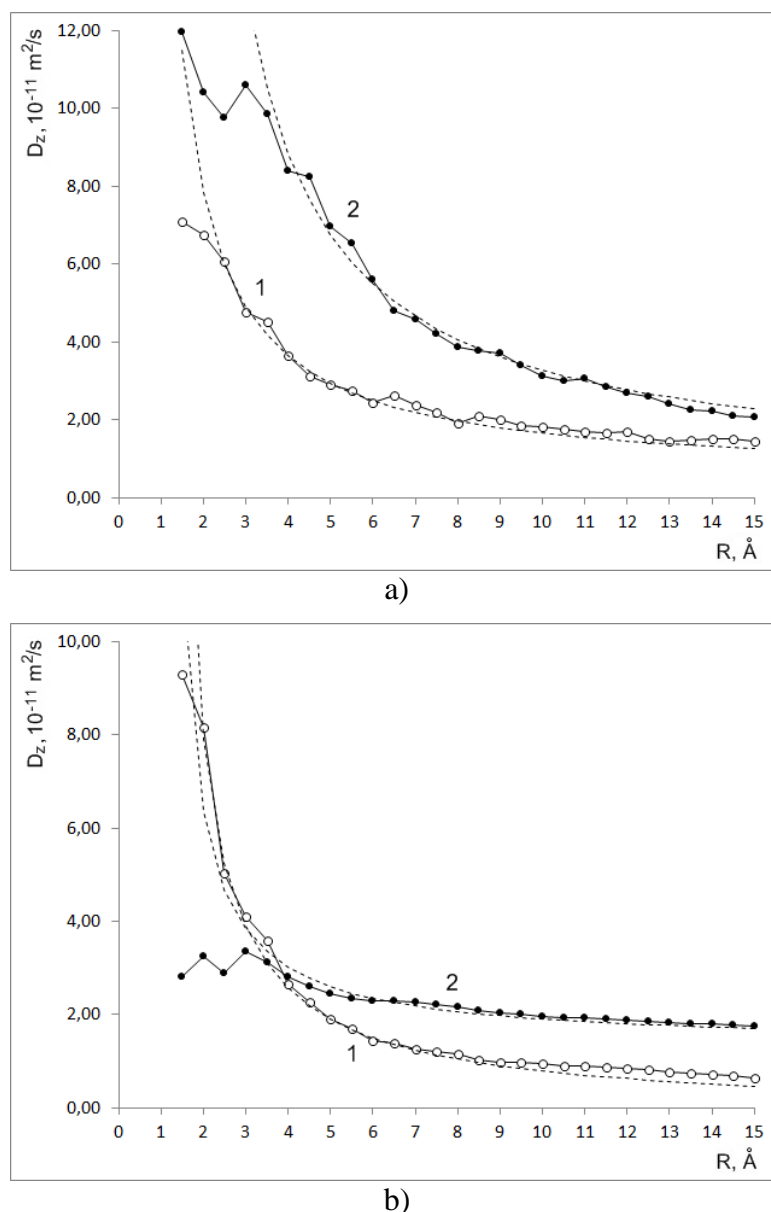


**Fig. 4.** Dependences of the self-diffusion coefficient along triple junctions of  $\langle 100 \rangle$  18°/18°/36° (a) and  $\langle 111 \rangle$  15°/15°/30° (b) tilt boundaries on radius  $R$  of the calculation area at temperature of 1500 K. 1 – additional vacancies were not introduced; 2 – 2% of conditional vacancies were introduced. Dashed line - approximation of  $c_1/(R+c_2)+c_3$  type.

Second, the values of the diffusion coefficient along the triple junctions containing excess free volume (dependences 2 in Fig. 4) in all cases were higher than the values obtained

in the case when additional vacancies were not introduced except values obtained at small radiuses of calculation area for the junctions of  $\langle 111 \rangle$  boundaries. This is explained, as already mentioned above, the relatively more "blurriness" of the junction of  $\langle 111 \rangle$  boundaries and diffusion channel.

The diffusion channel has no clear border, so to determine the size of it the obtained curves were complemented by theoretical curves at an assumption that the entire diffusion occurs only along the infinitely narrow grain boundaries and triple junction. In this case, the discrepancy of curves – the approximation and obtained in the model – will provide an opportunity to evaluate the effective radius of the triple junctions.

As an approximation curves the curves of  $c_1/(R+c_2)+c_3$  form were used, where  $c_1$ ,  $c_2$ ,  $c_3$  – constants. According to the search method of the diffusion radius of the triple junction, described in [10], the dependence  $D_z(R)$  should theoretically take the form of  $c_4/R$  or  $c_5/R^2$ , where  $c_4$  and  $c_5$  – some constants. The first dependence is obtained if triple junction represented as a simple connection of grain boundaries without any structural features, the second – if the triple junction has a substantially higher diffusive permeability compared with the grain boundaries. In our case neither the first nor the second formulas do not correctly described the main part of the received dependences. Therefore the form of approximation curves was little changed:  $c_1/(R+c_2)+c_3$ , where constants  $c_2$  and  $c_3$  were relatively small values. Such curves are well described the received in the computer model results. With the help of these curves is also easily can be identified the discrepancy model and theoretical results to determine the effective radius of triple junctions.

According to the dependences shown in Fig. 4 the diffusion radius of the considered junctions of  $\langle 100 \rangle$  and  $\langle 111 \rangle$  tilt boundaries did not contain specially introduced free volume is relatively small and equal 2-2,5 Å. This radius, however, corresponds to half of width of grain boundaries, which once again confirms the conclusions drawn in respect of such junctions, that they do not stand out against the background of their constituent grain boundaries [10]. The junctions obtained at introduction of 2% additional vacancies have a higher diffusion radius: the junctions of  $\langle 100 \rangle$  boundaries – about 3.5 Å, the junctions of  $\langle 111 \rangle$  boundaries – 4-5 Å. It should be noted that these results do not depend on the temperature at which the dependences  $D_z(R)$  were received.

#### 4. Conclusion

In the present study it was evaluated the diffusion radius of triple junctions of  $\langle 111 \rangle$  and  $\langle 100 \rangle$  tilt boundaries in Ni, obtained by crystallization, depending on the content of free volume. It is shown that diffusion in the area of triple junctions containing excess free volume proceeds much more intense than in the case when the additional vacancies were not introduced in the calculation block.

In the  $\langle 100 \rangle$  boundaries and junctions formed by them during crystallization the free volume dissipated much more efficiently than in the junctions formed by the  $\langle 111 \rangle$  boundaries. For this reason the diffusion radius of the triple junction of  $\langle 100 \rangle$  boundaries at the introduction of 2 % conditional vacancies (about 3.5 Å) less than the radius of the junction of  $\langle 111 \rangle$  boundaries (4-5 Å). In comparison with the obtained earlier in [6] energy radiuses the diffusion radiuses are substantially less: for junctions of  $\langle 100 \rangle$  tilt boundaries approximately two times, for junctions of  $\langle 111 \rangle$  boundaries approximately three times. The intensity of diffusion in a triple junction as a rule unevenly distributed and is higher in center of the channel.

#### Acknowledgment

*The reported study was partially supported by RFBR, research projects No. 16-48-190182-r\_a.*

**References**

- [1] G. Palumbo, K.T. Aust // *Scripta Metallurgica et Materialia* **24** (1990) 1771.
- [2] S.G. Protasova, V.G. Sursaeva, L.S. Shvindlerman // *Physics of the Solid State* **45** (2003) 1471.
- [3] A.I. Gusev // *Physics-Uspekhi* **41** (1998) 49.
- [4] P. Rodriguez, D. Sundararaman, R. Divakar, V.S. Raghunathan // *Chemistry for Sustainable Development* **8** (2000) 69.
- [5] G.M. Poletaev, D.V. Novoselova, V.M. Kaygorodova // *Solid State Phenomena* **249** (2016) 3.
- [6] G.M. Poletaev, D.V. Novoselova, V.M. Kaygorodova, I.V. Zorya, M.D. Starostenkov // *Fundamental'nye problemy sovremennogo materialovedenia* **13** (2016) 238. (In Russian).
- [7] F. Cleri, V. Rosato // *Physical Review B* **48** (1993) 22.
- [8] G.M. Poletaev, M.D. Starostenkov // *Technical Physics Letters* **29** (2003) 454.
- [9] M. Starostenkov, G. Poletaev, R. Rakitin, D. Sinyaev // *Materials Science Forum* **567-568** (2008) 161.
- [10] G.M. Poletaev, D.V. Dmitrienko, V.V. Diabdenkov, V.R. Mikrukov, M.D. Starostenkov // *Physics of the Solid State* **55** (2013) 1920.
- [11] L.N. Larikov, V.I. Isaychev, *Diffusion in metals and alloys* (Naukova dumka, Kiev, 1987).
- [12] T. Frolov, Y. Mishin // *Physical Review B* **79** (2009) 174110.
- [13] H. Gleiter, B. Chalmers, *High-angle grain boundaries* (Pergamon Press, New York, 1972).